Relative abundances of cosmic ray nuclei B-C-N-O in the energy region from 10 GeV/n to 300 GeV/n. Results from ATIC-2 (the science flight of ATIC).

A. D. PANOV[1], N. V. SOKOLSKAYA[1], J. H. ADAMS, JR.[2], H. S. AHN[3], G. L. BASHINDZHAGYAN[1], K. E. BATKOV[1], J. CHANG[4,5], M. CHRISTL[2], A. R. FAZELY[6], O. GANEL[3], R. M. GUNASINGHA[6], T. G. GUZIK[7], J. ISBERT[7], K. C. KIM[3], E. N. KOUZNETSOV[1], M. I. PANASYUK[1], W. K. H. SCHMIDT[5], E. S. SEO[3], J. WATTS[2], J. P. WEFEL[7], J. WU[3], V. I. ZATSEPIN[1].

[1]*Skobeltsyn Institute of Nuclear Physics, Moscow State University, Moscow, Russia* [2]*Marshall Space Flight Center, Huntsville, AL, USA* [3]*University of Maryland, Institute for Physical Science & Technology, College Park, MD, USA* [4]*Purple Mountain Observatory, Chinese Academy of Sciences, China* [5]*Max-Planck Institut for Solar System Research, Katlenburg-Lindau, Germany* [6]*Southern University, Department of Physics, Baton Rouge, LA, USA* [7]*Louisiana State University, Department of Physics and Astronomy, Baton Rouge, LA, USA*

panov@dec1.sinp.msu.ru

Abstract: The ATIC balloon-borne experiment measures the energy spectra of elements from H to Fe in primary cosmic rays from about 100 GeV to 100 TeV. ATIC is comprised of a fully active bismuth germanate calorimeter, a carbon target with embedded scintillator hodoscopes, and a silicon matrix that is used as a main charge detector. The silicon matrix produces good charge resolution for the protons and helium but only a partial resolution for heavier nuclei. In the present paper a charge resolution of ATIC device was essentially improved and backgrounds were reduced in the region from Be to Si by means of the upper layer of the scintillator hodoscope that was used as an additional charge detector together with the silicon matrix. The flux ratios of nuclei B/C, C/O, N/O in the energy region from about 10 GeV/nucleon to 300 GeV/nucleon that were obtained from new high-resolution and high-quality charge spectra of nuclei are presented. The results are compared with existing theoretical predictions.

Introduction

The ATIC spectrometer, the procedures of its calibration and the algorithm of trajectory of primary particles reconstruction have been described in [3, 9, 7]. Charge resolution provided by the silicon matrix is sufficient to obtain spectra of primary protons and helium [8, 6] and preliminary spectra of some abundant heavy nuclei [5, 6].

A very important sort of data to understand mechanisms of propagation of cosmic rays in the Galaxy is boron (which is secondary and not abundant nucleus) to carbon fluxes ratio in cosmic rays. The problem of B/C ratio have been widely experimentally investigated in the energy range 0.5–50 GeV/n (see [1] and references herein). The energy range of the ATIC experiment permits to obtain the data for the higher energies (up to 200–300 GeV/n). But there are obstacles to solve the problem: 1) too low charge resolution of the silicon matrix in the range of charges 5–8, 2) high backgrounds in the silicon matrix charge spectrum in the range of boron and carbon (see fig. 1). In this paper we use the upper layer of the scintillator hodoscope to improve charge resolution of the device and to reduce backgrounds in B-C region to solve B/C problem in the ATIC experiment.

Improved charge spectrum

The upper scintillator layer of the hodoscope is comprised by 42 parallel scintillator strips $1 \times 2 \times 88.2$ cm^3. The first task is to force these scintillators to work as a supplementary charge detector. This task includes a multi-step procedure of calibration of scintillators as a charge detector which

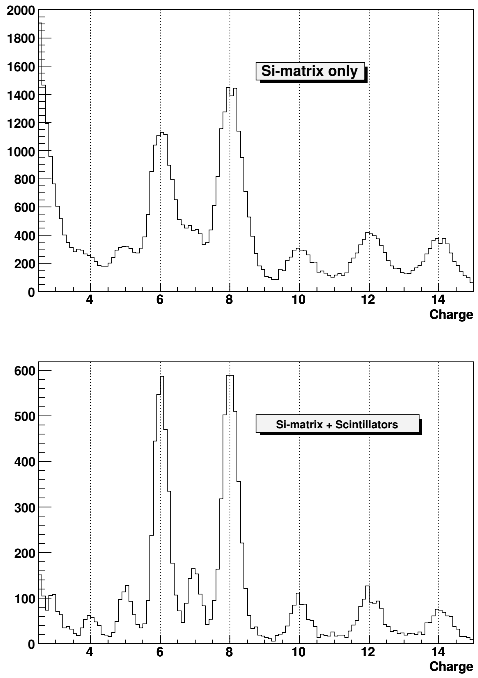

Figure 1: The charge spectra obtained with the silicon matrix only and with the silicon matrix plus the upper layer of hodoscope for the range of energy deposit in BGO calorimeter 50–100 GeV (primary energy per particle approximately 150–300 GeV)

will be described in details elsewhere. The method to improve charge spectrum by the charge detected by the upper layer of the scintillators hodoscope is the following. At the first step we use usual method to measure the charge of primary particle by the trajectory reconstructed from signals in BGO-calorimeter and by the charge detected with silicon matrix (Q_{Si}) by the maximal signal in the area of confusion for the trajectory as described in [3, 9, 7]. At the second step we find the charges detected in each scintillator strip and select the strip with the charge nearest to the charge detected by the silicon matrix (Q_{Sci}). The found charge is accepted if the distance from the strip to the reconstructed trajectory is less than 5cm and is rejected otherwise. At the third step Q_{Sci} is rejected if $|Q_{\text{Sci}} - Q_{\text{Si}}| > 0.25$. The final result for the charge is $Q = (Q_{\text{Sci}} + Q_{\text{Si}})/2$. The described procedure reduces the backgrounds in the charge spectrum and improves its resolution but reduces the initial statistics by the factor of about 4. There are other strategies to process charge data from the scintillator hodoscope but for this paper we select the strategy of “higher resolution - lower backgrounds - lower statistics”. The charge spectra obtained with the silicon matrix only and with the silicon matrix plus the upper layer of hodoscope are compared in fig. 1.

Measurement of the relative fluxes

We calculate ratio of fluxes of different nuclei in cosmic rays to the flux of carbon against energy of particles per nucleon. It is a multi-step procedure which is designed to obtain the most exact information for fluxes of nuclei with charges $4 \leq q \leq 14$.

1. For five ranges of the energy deposit E_d in the BGO calorimeter (50–100, 100–200, 200–398, 398–794, 794–1585 GeV) the charge spectra (similar to fig. 1, the lower graph) are builded up. There is a dependency of ionization from the energy of particles. To account for this dependency we decompose each charge spectrum by Gaussian peaks (the value χ^2 per one degree of freedom is close to 1 in all cases), calculate the positions of peaks and produce *charge boxes* for each particular primary particle such that the margins of boxes are at the half of path between adjacent peaks. The number of counts $I^0_{s,q}$ in each charge box q for E_d range number s is the raw data to obtain the fluxes of primary particles ($s = 0$ corresponds to the energy region of E_d 50–100 GeV, etc).

2. Protons and helium due to interaction in the substance (aluminum honeycomb and other) of the ATIC device above the silicon matrix could sometimes simulate heavier nuclei. This effect is energy dependent (grows with energy). Corresponding backgrounds $B^{\text{p,He}}_{s,q}$ for each value $I^0_{s,q}$ are calculated by simulation of propagation of protons and helium through the ATIC device by the FLUKA code [2], with simulation of the conditions of charge selection (see previous section). The apparatus charge line widths are accounted for as well. This procedure produces the corrected values of intensities $I^1_{s,q} = I^0_{s,q} - B^{\text{p,He}}_{s,q}$. The value of $B^{\text{p,He}}_{s,q}$ for boron ($q = 5$) varies from 9% to 36% of $I^0_{s,q}$.

3. The particles with charges $q \geq 15$ due to fragmentation in the substance of the ATIC device above the silicon matrix could simulate nuclei of $4 \leq q \leq 14$. The corresponding backgrounds were subtracted but the effect is small (about 0.1% for boron) and we do not describe the method of subtraction here.

4. Each nuclei of $4 \leq q \leq 14$ due to interactions in the ATIC device, and due to the apparatus broadening of lines produces some "charge response" of the device which may be described for each particular nucleus q at the entrance of the device by a set of the coefficients $K_4^q, K_5^q, \ldots, K_{14}^q$, where K_4^q is the probability to find nucleus q in the charge box 4, etc. Of course the coefficient K_q^q dominates strongly in the set $K_4^q, \ldots, K_{14}^q$. In other words the matrix $||K_{q'}^q||$ is diagonally-dominated. Let F_q be the intensity of the nucleus q at the entrance of the device. Then for each energy region s the experimental charge spectrum I_q^1 after subtraction of p-He backgrounds (described above in the item 2, we do not write the index s for simplicity) may be written as

$$\begin{array}{l} I_4^1 = K_4^4 F_4 + K_4^5 F_5 + \ldots + K_4^{14} F_{14} \\ \ldots\ldots\ldots\ldots\ldots\ldots\ldots\ldots\ldots\ldots \\ I_{14}^1 = K_{14}^4 F_4 + K_{14}^5 F_5 + \ldots + K_{14}^{14} F_{14} \end{array} \quad (1)$$

Eq. (1) is a square linear system relative to unknown values $F_4, F_5, \ldots, F_{14}$ with diagonally-dominated matrix and it can be easily solved by usual methods. The coefficients of the system $K_{q'}^q$ are calculated by simulation of propagation of different nuclei through the ATIC device with FLUKA and the values I_q^1 are already known after steps 2 and 3. The ratio of B/C (calculated as the ratio of the contents of the related charge boxes) reduces at the step 4 to 14%–42% for different energies (the effect is energy dependent).

5. The next step is a transition from the spectra of fluxes per region of E_d (see step 1) as a functions of E_d (it is the result of step 4) to the spectra of primary energy per nucleon. For each nucleus this procedure includes firstly a calculation of expected primary energy for each edge of the region of E_d (see step 1). To solve this problem FLUKA simulation of energy deposition was used with supposition of the primary differential momentum spectra to be power one with the index $\gamma = -2.6$ (there is only a weak dependence of exact value of γ in such a calculation). After normalization of the primary energy to the atomic weight and to the width of the related energy region it is occurred that the fluxes for different nuclei are connected with different energies. But one is interested for the ratio of fluxes at the same energy per nucleon for any species (it is the most physically meaningful quantity). To obtain the ratio of fluxes at the same energies we calculate the energy points obtained as a geometrical mean for the corresponding points for boron and carbon and calculate all fluxes for these energy points by interpolation of the spectrum of each nucleus. This procedure increases B/C ratio of the step 4 to 13%–23% (different for different energies).

6. The mean altitude of the flight of ATIC-2 was 36.5 km which corresponds to 4.87 g/cm^2 of the residual atmosphere. To obtain the primary fluxes of the species above the atmosphere the interaction of nuclei in the atmosphere should be accounted for. The interaction may be described as fragmentation of nuclei without changing of the energy per nucleon. Then the interaction for each primary energy and for each primary nucleus q may be described by a set of coefficients $L_{q'}^q, q' \leq q$ which show the probability to find the nucleus q' at the entrance of the device. The coefficients $L_{q'}^q$ were calculated by simulation of propagation of nuclei in the atmosphere by the FLUKA. Let ψ_q be the flux of nucleus q in the terms of energy per nucleon at the entrance of the device (these values are known after step 5; we omit the index of the energy for simplicity) and φ_q be the same values above the atmosphere for some definite energy per nucleon. Then one can write

$$\begin{array}{l} \psi_4 = L_4^4 \varphi_4 + \ldots + L_4^{14} \varphi_{14} + \varepsilon_4 \\ \ldots\ldots\ldots\ldots\ldots\ldots\ldots\ldots \\ \psi_{14} = L_{14}^{14} \varphi_{14} + \varepsilon_{14}, \end{array} \quad (2)$$

where $\varepsilon_4, \ldots, \varepsilon_{14}$ are small corrections related to the fragmentation of nuclei heavier than silicon ($q = 14$). This corrections are calculated approximately (we omit the details). If ε_q are known then the system (2) to be a square linear system relative to $\varphi_4, \ldots, \varphi_{14}$ with the triangle and diagonally-dominated matrix $L_{q'}^q$ and it can be solved directly starting from the final equation. The atmospheric correction reduces B/C ratio to 13%–33% for different primary energies.

Table 1: B/C, N/O, C/O ratio against primary energy per nucleon (GeV/n). The numbers in parenthesis give the uncertainty in the last significant digits quoted.

E	B/C	N/O	C/O
19.9	0.180(11)	0.219(10)	1.020(26)
38.3	0.169(15)	0.199(13)	1.087(43)
74.3	0.119(29)	0.184(24)	0.933(60)
149	0.156(53)	0.172(39)	0.934(105)
307	0.064(63)	0.144(68)	1.022(227)

The experimental errors were calculated as a combination of the Poisson dispersion of the experimental statistics and the statistical errors of the simulations. If the desired quantities were obtained as a solution of a linear system (as in steps 4 and 6) then corresponding complete covariation matrix were calculated by Monte Carlo method. All reported errors are the standard deviations.

Results and discussion

The results for B/C, N/C, O/C ratio are presented in table 1. The data for B/C ratio along with the data of HEAO-3-C2 experiment [1] and with theoretical predictions are shown in fig. 2 (lack of space precludes graphs for the other ratios). One can see that the data of present work is in a reasonable agreement with the data of [1] but are extended to higher energies. The theoretical curves in fig. 2 are calculations in leaky box approximation. The dashed line is based on the HEAO-3-C2 fit for the Galaxy escape length [1] $\lambda_{\text{esc}} = 34.1\beta R^{-0.60}$ g cm^{-2} (R is the rigidity) and the solid line is for the escape length obtained in the model of Kolmogorov type of magnetic turbulence and reacceleration during propagation [4]:
$\lambda_{\text{esc}} = 4.2(R/R_0)^{-1/3}\left[1 + (R/R_0)^{-2/3}\right]$ g cm^{-2}, where $R_0 = 5.5$ GV. Whereas the experimental data support general trend of decreasing B/C ratio with energy it is impossible to distinguish between different models of propagation of particles due to large experimental errors.

It should be noted that our experimental data are model dependent due to extensive simulation of rather high background by the FLUKA system, but the situation may be improved by usage of additional simulation codes. One can expect that the experimental separation between different models of propagation would be possible with some additional experiments.

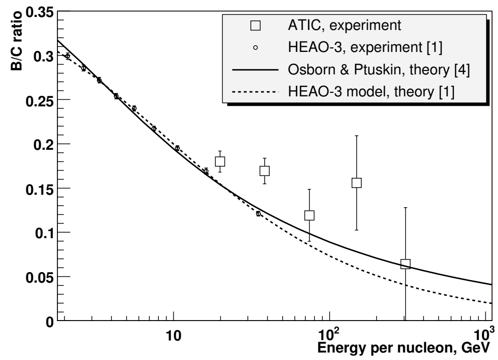

Figure 2: B/C ratio from this work, from HEAO-3-C2 experiment and from theory.

Acknowledgements. This work was supported by RFBR Grant 05-02-16222 in Russia and NASA Grants Nos. NNG04WC12G, NNG04WC10G, NNG04WC06G in the USA.

References

[1] J. J. Engelmann et al. (HEAO Collaboration). *Astron. Astrophys.*, 233:96, 1990.

[2] A. Fassò et al. arXiv:hep-ph/0306267, 2003.

[3] T. G. Guzik et al. (ATIC Collaboration). *Adv. Sp. Res.*, 33(10):1763, 2004.

[4] J. L. Osborn and V. S. Ptuskin. Sov. Astron. Lett. 14(2):132, 1988.

[5] A. D. Panov et al. (ATIC Collaboration). *Adv. Sp. Res.*, 37:1944, 2006.

[6] A. D. Panov et al. (ATIC Collaboration). *Bull. Russ. Acad. Sc.: Physics*, 71:494, 2007.

[7] N. V. Sokolskaya et al. *Phys. Atom. Nucl.*, 68:1176, 2005.

[8] J. P. Wefel et al. (ATIC Collaboration). In *29th ICRC*, V.3, P.105, 2005.

[9] V. I. Zatsepin et al. (ATIC Collaboration). *Nucl. Instr. Meth. A*, 524:195, 2004.